NRC Research Press

ARTICLE

Combining aerial LiDAR and multispectral imagery to assess postfire regeneration types in a Mediterranean forest

Santiago Martín-Alcón, Lluís Coll, Miquel De Cáceres, Lídia Guitart, Mariló Cabré, Ariadna Just, and José Ramón González-Olabarría

Abstract: Wildfires play a major role in driving vegetation changes and can cause important environmental and economic losses in Mediterranean forests, especially where the dominant species lacks efficient postfire regeneration mechanisms. In these areas, postdisturbance vegetation management strategies need to be based on detailed, spatially continuous inventories of the burned area. Here, we present a methodology in which we combine airborne LiDAR and multispectral imagery to assess postfire regeneration types in a spatially continuous way, using a Mediterranean black pine (*Pinus nigra* Arn ssp. *salzmannii*) forest that burned in 1998 as a case study. Five postfire regeneration types were obtained by clustering field-plot data using Ward's method. Two of the five regeneration types presented high tree cover (one clearly dominated by hardwoods and the other dominated by pines), a third type presented low to moderate tree cover, being dominated by hardwoods, and the remaining two types matched to areas dominated by soil–herbaceous or shrub layers with very low or no tree cover (i.e., very low to no tree species regeneration). These five types of regeneration were used to conduct a supervised classification of remote sensing data using a nonparametric supervised classification technique. Compared with independent field validation points, the remote sensing based assessment method resulted in a global classification accuracy of 82.7%. Proportions of regeneration types in the study area indicated a general shift from the former pine-dominated forest toward hardwood dominance and showed no serious problems of regeneration failure. Our methodological approach appears to be appropriate for informing postdisturbance vegetation management strategies over large areas.

Key words: postfire regeneration types, remote sensing data, wildfire effects, postdisturbance management, *Pinus nigra*.

Résumé : Les feux de forêt jouent un rôle déterminant dans la composition de la végétation et peuvent causer d'importantes pertes économiques et environnementales dans les forêts méditerranéennes, particulièrement dans les endroits où les espèces dominantes n'ont pas de mécanismes efficaces de régénération après feu. Dans ces endroits, les stratégies de gestion de la végétation après feu doivent être fondées sur des inventaires détaillés et continus dans l'espace des zones brûlées. Nous présentons ici une méthodologie qui combine le lidar aéroporté et l'imagerie multispectrale pour évaluer les types de régénération après feu de manière continue dans l'espace, en utilisant comme étude de cas une forêt de pin de Salzmann (*Pinus nigra* Arn. ssp. *salzmannii*) qui a brûlé en 1998. Cinq types de régénération après feu ont été obtenus en regroupant les données de placettes sur le terrain à l'aide de la méthode de Ward. Deux des cinq types de régénération avaient une fort couvert d'espèces arborescentes dominé dans un cas par des feuillus et dans l'autre par des pins; un troisième type avait un couvert arboré faible à modéré dominé par des feuillus; les deux derniers types correspondaient aux régions dominées par des strates herbacées ou arbustives où la régénération arborescente était très faible ou inexistante. Ces cinq classes ont été utilisées pour effectuer une classification dirigée des données de télédétection à l'aide d'une technique de classification dirigée non paramétrique. Comparativement à des points de contrôle indépendants sur le terrain, la classification de la méthode d'évaluation fondée sur la télédétection avait une précision globale de 82,7 %. La proportion des types de régénération dans la zone d'étude indiquait qu'il y avait une évolution générale de la forêt jadis dominée par les pins vers une dominance des feuillus et ne révélait aucun problème sérieux de régénération. Notre approche méthodologique semble appropriée pour appuyer les stratégies de gestion de la végétation à la suite d'une perturbation sur de vastes superficies. [Traduit par la Rédaction]

Mots-clés : types de régénération après feu, données de télédétection, effets des feux de forêt, gestion postperturbation, *Pinus nigra*.

Introduction

Wildfires have been the most important natural disturbance in Mediterranean ecosystems since at least the late Quaternary (Carrión et al. 2010; Pausas et al. 2008). In the Mediterranean region, humans have lived with fire and used it in their agricultural and rural activities for millennia. However, in the last midcentury, there has been an increase in the number of ignition sources, causing an increase in fire risk and in the frequency of uncontrolled fires (Gonzalez-Olabarria and Pukkala 2007; San-Miguel-Ayanz et al. 2013; Schelhaas et al. 2003). This increase has been attributed to a combination of factors that are related to, among others, land abandonment, the increase in the number of days with extreme fire hazard weather, and the increasing number of human-related ignition sources (Loepfe et al. 2010). In the Iberian Peninsula, large wildfires (>500 ha) have hit almost every type of forest ecosystem over the last decades, representing almost one-half of the total

Received 5 October 2014. Accepted 24 February 2015.

S. Martín-Alcón, L. Guitart, and J.R. González-Olabarría. Forest Sciences Center of Catalonia (CEMFOR-CTFC), Solsona 25280, Spain.
L. Coll and M. De Cáceres. Forest Sciences Center of Catalonia (CEMFOR-CTFC), Solsona 25280, Spain; Centre for Ecological Research and Forestry Applications (CREAF), Cerdanyola del Valles, 08193, Spain.
M. Cabré and A. Just. Institut Cartogràfic i Geològic de Catalunya (ICGC), Barcelona 08038, Spain.
Corresponding author: Santiago Martín-Alcón (e-mail: santiago.martin@ctfc.es).

Published at www.nrcresearchpress.com/cjfr on 26 February 2015.

burnt area during this period (Cubo María et al. 2012). This scenario of increased fire impacts may be further magnified in the future, as climate forecasts point to prolongation of droughts and hot spells, which are likely to further aggravate forest fire risk (Keenan et al. 2011; Lindner et al. 2010; Piñol et al. 1998; Resco de Dios et al. 2006).

In addition to changes in fire frequency and extent, some areas have suffered an increase in the occurrence of high-intensity crown fires, affecting forest types that had not historically been subject to fires such as the montane (sub-Mediterranean) forests dominated by Mediterranean black pine (*Pinus nigra* Arn ssp. *salzmannii*) or Scots pine (*Pinus sylvestris* L.) (Ordoñez and Retana 2004; Pausas et al. 2008; Vilà-Cabrera et al. 2012). These pine species lack direct postfire regeneration mechanisms and usually show almost no regeneration after crown fires (Pausas et al. 2008). In these areas, substitution of the pines by resprouting hardwoods (mostly *Quercus* species) is generally observed when the latter were present in the understory of the burnt stands (Puerta-Piñero et al. 2011; Rodrigo et al. 2004). In the particular case of *P. nigra* forests, the thick bark and high self-pruning ability of this species allow for the persistence of some surviving trees in the form of small islands interspersed across the burned landscape (Roman-Cuesta et al. 2009). The existence of such islands, together with the moderate shade tolerance of this species (Niinemets and Valladares 2006), may lead to greater opportunities for its mid- to long-term colonization of the burned area. In contrast, in the areas without the presence of sprouting species or remaining trees, important problems of soil recovery by woody vegetation are likely to arise, leading to increased soil erosion and forest degradation and causing long-term environmental and economic damage (Selkimäki et al. 2012).

Several factors inherent to forests in the Mediterranean basin such as the small size of forest ownership, slow growth rate due to limited water availability, or the dominance of mountainous terrain raise the cost of forestry operations and hamper the development of management actions (European Forest Institute (EFI) 2010; Gonzalez-Olabarria et al. 2008), including postfire restoration measures (Espelta et al. 2003*a*). These impediments may be, in part, tempered if detailed, spatially continuous assessments directed to classify the burned area by regeneration success, vegetation types, and (or) management are available (Vallejo et al. 2012). However, the extent of these types of disturbances makes these detailed, spatially continuous assessments often unattainable through field data gathering. Thus, the general approach that is used to run postfire assessments usually involves implementing a statistical sampling design to decide the location of inventory plots (Pausas et al. 2004; Proença et al. 2010; Puerta-Piñero et al. 2012; Shatford et al. 2007) and then applying modeling (i.e., extrapolation) techniques. The use of remote sensing (RS) data has recently emerged as an efficient alternative to provide adequate regeneration assessments over large areas that are affected by forest disturbances. In this line, some recent studies have used indicators like the normalized difference vegetation index (NDVI) (Tucker 1979), extracted from satellite imagery, to evaluate short-term regeneration success and recovery rates in terms of the total plant cover (Belda and Meliá 2000; Diaz-Delgado et al. 2003; Gouveia et al. 2010; van Leeuwen et al. 2010; Viedma et al. 1997; Vila and Barbosa 2010), even distinguishing the cover of woody shrubs or tree species regeneration (Riaño et al. 2002; Vicente-Serrano et al. 2011).

From an operational point of view, the value of these postdisturbance regeneration assessments might significantly increase if they were complemented with data that described the structure of the vegetation (e.g., relative cover of the different strata or functional groups, etc.). In relation to this, light detection and ranging (LiDAR) has recently emerged as a powerful tool for characterizing such structural attributes (Lefsky et al. 2002; Wulder et al. 2012) and holds great potential for evaluating medium- to long-term postdisturbance regeneration (Debouk et al. 2013; Johnstone et al. 2004). Combining LiDAR data with multispectral images could further improve the assessment of postfire vegetation by making it possible to accurately characterize low-vegetation attributes (Erdody and Moskal 2010; Riaño et al. 2007) and to identify individual tree species (Hill et al. 2010; Holmgren et al. 2008; Waser et al. 2011). It also enables the identification of vegetation typologies (Bork and Su 2007; Goetz et al. 2010; Mutlu et al. 2008), which may be especially appropriate in the case of low-resolution data. Typological characterization of forest stands for management purposes has been widely used on adult forest stands (e.g., Aubury et al. 1990; Herbert and Rebeirot 1985; Martin-Alcon et al. 2012; Reque and Bravo 2008), providing detailed, objective classifications of the stands according to their structural and floristic attributes. In the case of regenerating forest stands, such attributes are expected to largely influence the long-term dynamics of the forest and its accompanying ecosystem services (Elmqvist et al. 2003).

The aim of this study was to develop and test a simple, cost-effective methodology for conducting a detailed, spatially continuous characterization of postfire regeneration (i.e., recovery of vegetation cover) from widely available RS data, using a large forest fire in the Mediterranean basin as a case study. To this purpose, we defined and mapped the main postfire regeneration types in the study area using a combination of low-resolution airborne LiDAR data (useful for characterizing the three-dimensional structure of plant canopies) and NDVI data, computed from multispectral data from aerial images, potentially suitable for differentiating between species groups with different spectral signatures. We applied this methodology to the particular case of a large wildfire in a Mediterranean zone, but we anticipate that it could be easily adapted to assess vegetation responses to other forest disturbances and a wide range of forest ecosystems such as large-scale disease outbreaks or windthrow events.

Material and methods

The methodological approach adopted to assess postfire regeneration types based on RS data can be summarized in the following steps: (*i*) RS data processing (raw LiDAR data and raw imagery data), (*ii*) establishment and measurement of a set of field inventory plots located in two subsets of the study area (training areas), (*iii*) selection of the most informative RS variables to be used as candidate predictors, (*iv*) definition of alternative postfire regeneration typologies based on training field data, (*v*) selection of a regeneration typology on the basis of the classification accuracy of a supervised classification model using RS variables, (*vi*) extrapolation of the regeneration typologies to the whole study area through the application of the corresponding supervised classification model, and (*vii*) validation of the resulting classification using a set of observation points randomly located across the study area (validation stands) (Fig. 1).

Study area

The study was conducted in an area affected by a large forest fire in the central region of Catalonia (northeastern Spain). This wildfire burned nearly 24 000 ha in 1998 (Fig. 2), leading to almost complete loss of forest cover (Rodrigo et al. 2004). Prior to the wildfire, the area was composed of the typical Mediterranean mosaic-like landscape, with cultivated lands and scrublands (7700 ha and 2000 ha, respectively) interspersed with forest areas (14 000 ha). According to data in the Forest Ecological Inventory of Catalonia (Burriel et al. 2004), the dominant species before the wildfire was black pine, which covered 75% of the total forest surface. Aleppo pine (*Pinus halepensis* Mill.) was the second most abundant species, covering 15% of the forest surface. Both black pine and aleppo pine forests appeared as pure stands or as two-layered stands in which pine dominated the overstory and resprouting hardwoods dominated the understory (Fig. 2). The

Fig. 1. Flowchart depicting schematically the methodological approach. Numbers indicate the step order.

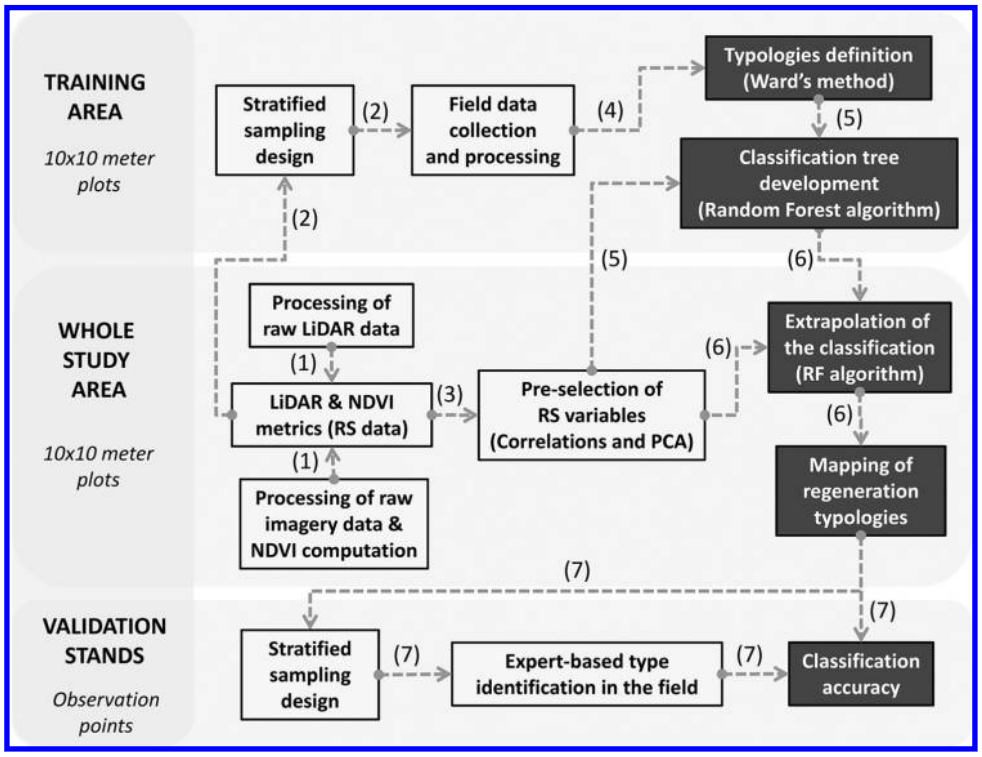

Fig. 2. Location and boundaries of (*a*) the wildfire location in the Iberian Peninsula and Catalonia region, (*b*) the study area and the calibration areas within the wildfire zone, (*c*) the dominant forest types in the study area before the 1998 wildfire (Centre for Ecological Research and Forestry Applications (CREAF) 1993; Dirección General de Conservación de la Naturaleza (DGCN) 2001), and (*d*) the field plots and the validation stands within the study area.

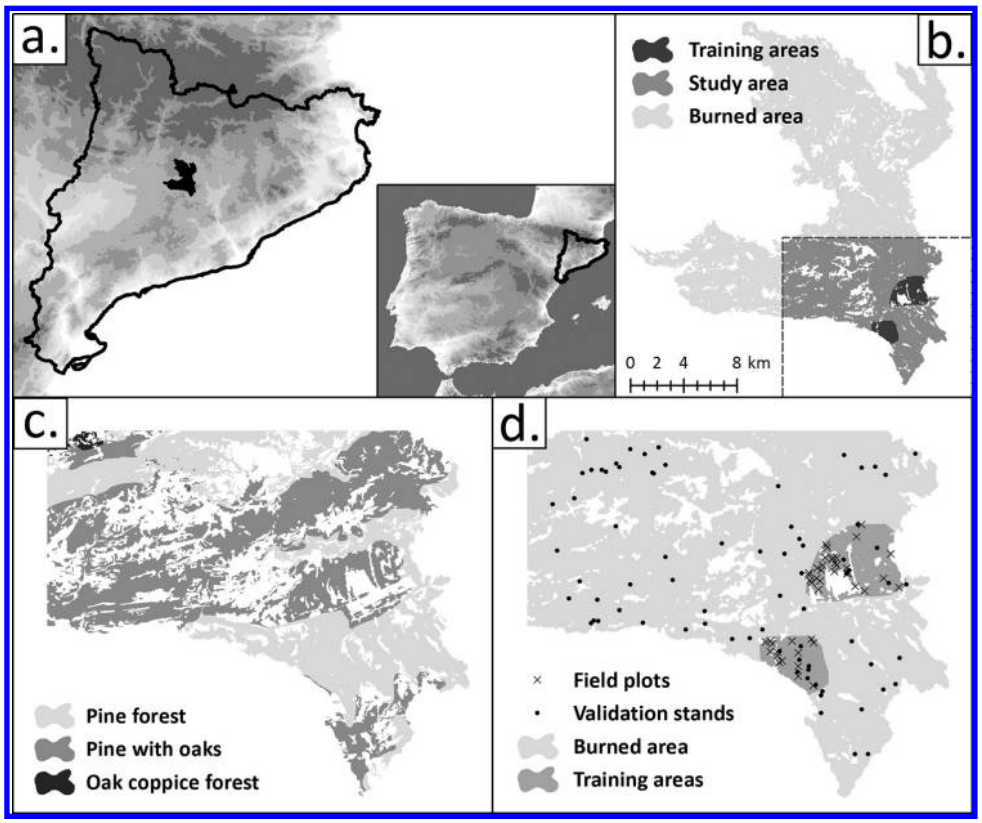

remaining forest surface was mainly covered by mixed hardwoods (mainly *Quercus ilex* L. and *Quercus cerrioides* Willk. & Costa) and *Pinus sylvestris* L. stands. The area presents a gentle relief with low hills ranging in elevation from 480 to 910 m above sea level (a.s.l.) and a dry–subhumid to subhumid Mediterranean climate, according to the Thornthwaite index.

From the total forest area that was affected by the 1998 wildfire, we selected a portion of 3973 ha that had burned at high severity (i.e., with no remaining adult trees) (Fig. 2). Areas affected by roads, agricultural fields, and other nonforest uses were excluded from the analysis, leaving a total of 3192 ha to be used for the postfire regeneration assessment. Additional criteria to determine the study area were the characteristics of the available RS data, as a minimum seasonal similarity in both LiDAR data and aerial images was required to avoid potential mismatches due to the use of data from different seasons (e.g., before and after budbreak in broadleaves). In our particular case, the LiDAR data were taken in the early summer of 2009 and the aerial photographs were taken in the early spring of 2011.

LiDAR data acquisition and processing

LiDAR data were acquired via the LidarCAT project (Cartographic and Geological Institute of Catalonia). The entire study area was covered by seven flight lines, and data were captured with an ALS50 II LiDAR sensor that was mounted on a Cessna Caravan 208B aircraft. The flight dates ranged from 30 May 2009 to 3 June 2009. The mean first-return point density of these LiDAR data was 0.5 pulses·m^{-2}, and each pulse captured up to four returns. LiDAR point coordinates were adjusted according to the methodology proposed by Kornus and Ruiz (2003). After filtering the clouds, low-intensity returns, and air points, LiDAR returns were automatically classified with the TerraScan ground classification routine (Terrasolid 2012) to differentiate ground from nonground returns. Ground routine classified ground points by iteratively building a triangulated surface model. The routine started by selecting some local low points that are confident hits on the ground. It was assumed that any 40 m × 40 m area would have at least one hit on the ground and that the lowest point would be a ground hit. This routine built an initial model and started molding the model upwards by iteratively adding new laser points to it. Each added point made the model follow the ground surface more closely. Iteration parameters of angle (4°) and distance (1 m) determined how close a point must be to a triangle plane to be accepted as a ground point and added to the model. The remaining nonground points were visually inspected and manually classified to extract wires and towers (as the low point density of the LiDAR data advised against the implementation of automatic algorithms for this purpose). Building roofs were extracted automatically using a new routine that classified nonground points that formed a planar surface of at least 40 m^2. Finally, the remaining nonground returns were classified as vegetation, and LiDAR height was replaced by its vertical distance to a triangular irregular network generated from ground returns.

The LiDAR vegetation point cloud was analyzed in a 10 m × 10 m regular grid with the FUSION software system (McGaughey and Carson 2003) to obtain structured statistical information on the laser returns. A height of 0.15 m, predefined from the vegetation field inventory, was used as a threshold to separate woody and shrubby vegetation from herbaceous vegetation and bare soil. Intensity data were normalized by the range normalization to a user-defined standard range (Donoghue et al. 2007; García et al. 2010):

$$(1) \qquad I' = I\frac{R^2}{R_S^2}$$

where I' is the normalized intensity, I is the raw intensity value, R is the range (LiDAR sensor–target distance), and R_S is the standard range (in this case, 2225 m, which corresponds to the mean range in the study area). This method eliminated the effect of path length variations on the intensity recorded by the system, providing values equivalent to the intensity that would have been recorded if all points were at the same range. The exact value of the range was not available for each LiDAR point; therefore, it was approximated by the use of the difference between the mean altitude of the flight and the elevation of each point and the projected distance between the point and the flight line. This approach should cause smaller errors than the option of using the altitude difference instead of the actual range (Coren and Sterzai 2006; Kukko et al. 2008). Only the first echoes that were returned from the aboveground vegetation were used for computing a set of LiDAR height and intensity metrics suitable to characterize forest vegetation structure and floristic composition (e.g., Donoghue et al. 2007; García et al. 2010; Holmgren et al. 2008; Latifi et al. 2012; Morsdorf et al. 2006). These metrics were the following: (*i*) percentiles of pulse height (H_P05, H_P10, H_P20, …, H_P80, H_P90, and H_P95) and pulse intensity (Int_P05, Int_P10, Int_P20, …, Int_P80, Int_P90, and Int_P95); (*ii*) mean (H_MEAN and Int_MEAN), mode (H_MODE and Int_MODE), standard deviation (H_SD and Int_SD), coefficient of variation (H_CV and Int_CV), interquartile range (H_IQ and Int_IQ), skewness (H_Sk and Int_Sk), and kurtosis (H_Kur and Int_Kur) of both pulse height and pulse intensity values. In addition, the following three ratios were generated: percentage of vegetation points (height > 0.15 m) in relation to all first returns (FR_VEG), percentage of vegetation points in relation to all returns (AR_VEG), and percentage of first returns above the mean (FR_abMEAN) and the mode (FR_abMODE) height.

Multispectral image acquisition and processing

NDVI imagery were obtained from the Cartographic and Geological Institute of Catalonia annual coverage flights at a ground sample distance of 22 cm and were generated from aerial photos with RGB (red, green, and blue) and near-infrared bands. The aerial photos were taken between 2 April 2011 and 10 April 2011 with digital mapping cameras (DMCs) DMC-26 and DMC-14 and were later orthorectified without stitching. The implemented procedure to produce NDVI from DMC imagery used the original DMC LR4 series files (low-resolution multispectral bands) with absolute radiometric calibration and was based on the manufacturer's calibration of the DMC, following the methodology proposed by Martínez et al. (2012). Radiance values from the red and near-infrared bands and their respective reflectances (i.e., ratio between incoming energy from the sun and reflected energy modulated by some geometric factors such as location, date, and time of exposure during acquisition) were obtained for each pixel using the following equations:

$$(2) \qquad R = \frac{\pi L_R}{\mu E_0}$$

$$(3) \qquad \mathrm{NIR} = \frac{\pi L_{\mathrm{NIR}}}{\mu E_0}$$

where R and NIR correspond to the reflectance values of each pixel from the red and the near-infrared bands, respectively, L_R and L_{NIR} are radiance values from the red and the near-infrared bands, μ is a geometric factor, and E_0 is the extraterrestrial solar radiation. Then, NDVI was calculated using the following equation:

$$(4) \qquad \mathrm{NDVI} = \frac{(\mathrm{NIR} - R)}{(\mathrm{NIR} + R)}$$

NDVI values were then aggregated to match the same 10 m × 10 m grid as used to aggregate the LiDAR data, and a set of NDVI statistics potentially suitable to describe regeneration structure and composition was calculated. For the NDVI distribution, the quartiles (NDVI_Q1, NDVI_Q2, and NDVI_Q3), interquartile range (NDVI_IQ), mean (NDVI_MEAN), coefficient of variation (NDVI_CV), and standard deviation (NDVI_SD) were obtained. NDVI values in the regenerating area generally ranged between 0 and 0.6. On this basis, the portion of each 10 m × 10 m cell presenting NDVI values within a variety of subranges were computed, using 0.05 increments (0.15–0.2, …, 0.55–0.6), 0.10 increments (0.15–0.25, …, 0.45–0.55), and 0.15 increments (0.15–0.3, 0.3–0.45, and 0.45–0.6) to maximize the chance of differentiating species or groups of species based on their different NDVI values.

Field data gathering

A field inventory was performed to define postfire regeneration types. The inventory consisted of a set of forty-four 10 m × 10 m plots placed along two sub-areas that were considered to be representative of the overall study area (hereafter training areas) (Fig. 2). Stratified random sampling was applied to capture the range of regeneration patterns in the training areas. For this purpose, LiDAR variables that were expected to describe plant height distribution and the distance to unburned patches were used to ensure that we covered both the structural (relative abundance of trees) and compositional (as pines are expected to be more abundant near the unburned patches) gradients characterizing the postfire vegetation. For each plot, a set of variables describing the floristic composition and aboveground biomass structure were measured. These were the percentage of the plot area covered by soil or herbs (%SOIL), low shrub species (0.15–0.5 m tall; %LOW SHRUBS), high shrub species (>0.5 m tall; %HIGH SHRUBS), pine regeneration (%PINES), and tree species regeneration (i.e., refers to all trees species, including pines; %TREES). Low and high shrub covers were later summed as %SHRUBS. We also measured mean height (cm) of all tree species (HTREES), pines (HPINES), and hardwoods (HHW). To improve the accuracy of the measured vegetation variables, each 10 m × 10 m plot was subdivided into 2.5 m × 2.5 m subplots. The variables were measured at the subplot level and converted into plot-level values by averaging the values of the measured subplots within each plot.

RS data reduction

A first preselection of the 64 LiDAR- and NDVI-derived variables that were initially considered was executed to avoid using redundant variables as candidate predictors. Principal component analysis with a Varimax rotation was executed on the whole set of RS data to identify groups of highly collinear variables. In parallel, we computed Pearson correlation coefficients to measure the associations between RS variables and the list of forest variables measured in the field plots. A total of 14 variables from the original 64 variables were finally preselected. These variables were the ones showing the highest correlation with field variables among each group of highly collinear variables (i.e., variables with very similar principal component analysis factor loadings). They comprised five height metrics (coefficient of variation, kurtosis, 10th and 95th percentile height, percentage of first returns of vegetation, and percentage of first returns above the mode of the height distribution), three LiDAR intensity metrics (standard deviation and 50th and 90th percentile intensities), and five NDVI-derived variables (1st quartile NDVI and percentage of plot with NDVI between 0.45 and 0.5, between 0.25 and 0.35, between 0.15 and 0.3, and between 0.45 and 0.6).

Definition of postfire regeneration types

A subset of the variables measured in the field (%SOIL, %PINES, and %TREES) was deemed sufficient to define postfire regeneration types, as they described the distribution of the plot cover among the main strata (soil–herbs, trees, and indirectly, shrubs) and the main floristic groups of the tree layer (pines and hardwoods). The 44 training plots were clustered according to their squared Euclidean distances using Ward's hierarchical method (Ward 1963) based on these variables. Several alternative partitions of the resulting dendrogram (i.e., those exhibiting high between-group distance (Hair et al. 2009) and strong ecological rationale) were saved.

Development of the classification model

We used preselected RS variables from the field plots and the Random Forest (RF) classification algorithm (Breiman 2001) to evaluate the different partition alternatives and to obtain a model for the classification of the whole study area. RF is a nonparametric, supervised classification technique that has shown good performance in classifying remotely sensed data (e.g., Falkowski et al. 2009; Hudak et al. 2012). The RF technique uses a bootstrap approach for achieving higher accuracies while simultaneously addressing overfitting problems associated with traditional classification tree models. A large number of classification trees are produced from a random subset of training data (approximately 63% for a random subset), permutations are introduced at each node, and the most common classification result is selected. We ran each RF model with 5000 bootstrap replicates (i.e., individual classification trees). With the goal of avoiding bias in the prediction caused by imbalanced classes, the number plots per class in bootstrap samples was equal to the number of plots of the less frequent class (Evans and Cushman 2009). Out-of-bag (OOB) error estimates were calculated for each tree by classifying the portion of training data not selected in the bootstrap sample, and overall accuracy was calculated by averaging error rates across all trees in the model; this is analogous to cross-validated accuracy estimates (Cutler et al. 2007).

A model-selection procedure (i.e., variable reduction) was employed to select the optimal RS variables to use in the classification of postfire regeneration types. The procedure was formulated to develop the most parsimonious classification model while retaining the highest possible classification accuracy. We ran a RF model-selection function that uses model improvement ratio (MIR) standardized importance values (Evans et al. 2011; Evans and Cushman 2009) to objectively choose the most important RS variables for predicting the regeneration type of each plot. The MIR uses the permuted variable importance, represented by the mean decrease in OOB error, standardized from zero to one. The variables were subset using 0.10 threshold increments on the original model's variable importance, with all variables above the threshold retained for each model. Each subset model was compared, and the model that exhibited the lowest total OOB error and lowest maximum within-class error was selected. After selecting the best model for each one of the different alternative partitions, we determined the final regeneration typology as that whose classification model had obtained the highest classification accuracy. For this study, the RF algorithm was implemented using the RandomForest package (Liaw and Wiener 2002) in the R statistical program (R Development Core Team 2007).

Mapping of regeneration types and field-based validation

Each 10 m × 10 m plot in the study area was classified into one of the regeneration types by applying the final classification model on the RS variables. Regeneration types were then mapped and a set of landscape metrics were generated for explaining the spatial configuration of the landscape according to the distribution of regeneration patches. These size- and shape-related metrics were the area and percentage covered by each regeneration type, the percentage of the type area by patch size classes, the mean patch size (PS_m) and its coefficient of variation (PS_{cv}), and the mean shape index (MSI), as defined by Rempel et al. (2012).

Table 1. Descriptive statistics (mean (standard deviation)) of the main field variables for each of the regeneration types obtained in the five-type classification generated by Ward's clustering method.

Type	*n*	%SOIL	%LOW SHRUBS	%HIGH SHRUBS	%TREES	%PINES	H_HW	H_PINES
1	5	54.11 (10.21)	39.11 (10.91)	3.21 (1.21)	3.61 (5.31)	0.41 (0.31)	84.31 (111.61)	55.91 (62.71)
2	5	28.71 (5.01)	39.91 (18.51)	24.41 (19.21)	7.01 (4.51)	1.91 (2.71)	125.61 (116.71)	130.91 (125.91)
3	11	26.61 (6.61)	28.41 (11.11)	10.11 (7.31)	34.91 (7.81)	7.71 (7.81)	272.41 (104.31)	122.61 (71.01)
4	10	14.81 (6.11)	17.41 (6.51)	14.71 (13.31)	53.11 (9.51)	6.61 (6.81)	361.61 (67.91)	119.81 (60.41)
5	13	13.71 (5.81)	20.91 (14.31)	8.51 (9.51)	57.01 (17.31)	45.41 (16.51)	215.51 (145.51)	206.11 (53.61)

Note: For definitions of main field variables, see Materials and methods for variable definitions.

Fig. 3. Schematic interpretation of the 56 postfire regeneration types obtained from Ward's clustering method. Regeneration types are as follows: type 1, defective cover of woody vegetation; type 2, dominance of shrub cover; type 3, hardwoods, low–moderate cover; type 4, hardwoods, high cover; type 5, pines, moderate–high cover.

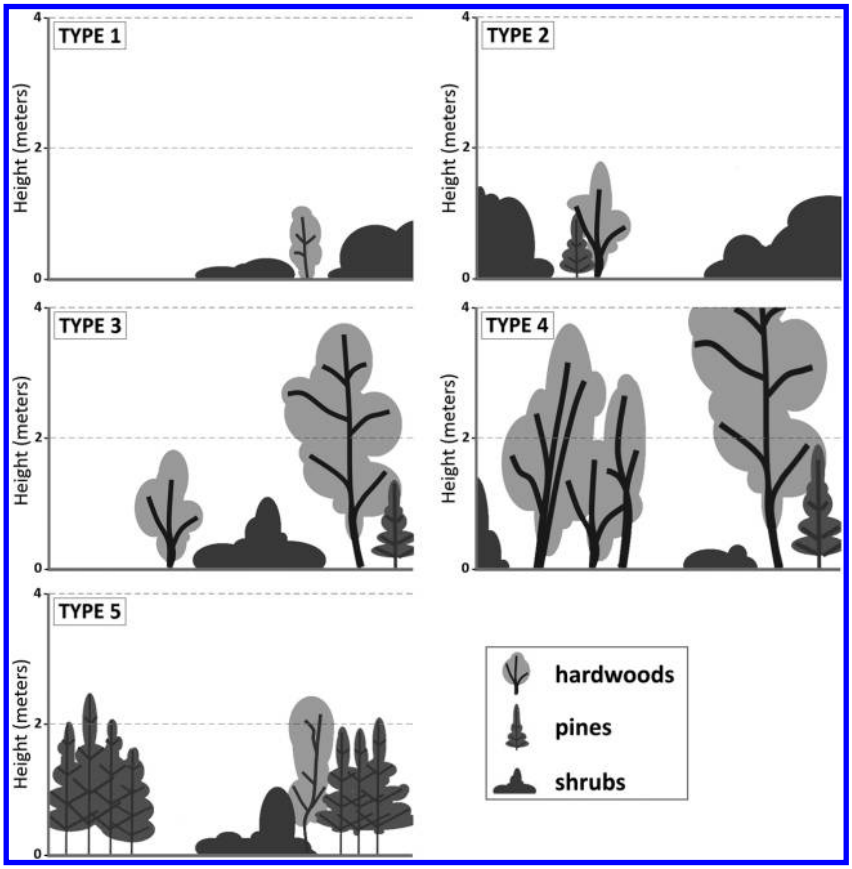

The validity of the final classification for the whole study area was evaluated by comparing the regeneration type assignations made from the supervised classification of RS data (using the classification model generated by RF) with visual assessments obtained in the field. For this purpose, 15 sampling points per regeneration type were distributed along the study area using stratified random sampling (Fig. 2). An independent user was asked to assign each of these stands to one of the regeneration types, based on a visual examination of the stand characteristics, using the type descriptions in terms of forest variables (see Table 1 and Fig. 3) as a guide. Measures of height and cover of the different vegetation strata were taken when visual estimation was not obvious. Finally, a confusion matrix was generated to estimate the accuracy of the RS-based assignations with respect to the visually based assignments.

Results

Postfire regeneration typologies

The dendrogram resulting from the application of Ward's clustering method on the variables measured in the 44 field plots (see Supplementary Figure S1[1]) led to three possible choices for the placement of the cut-off point of the hierarchical tree (i.e., three partition alternatives), creating a four-type, five-type and six-type partitions. By comparing the classification accuracy of the models developed using RF for the four-, five-, and six-type partitions, we found the five-type partition to be the best in terms of overall accuracy, with 79.55% of the plots being correctly classified (i.e., OOB error estimate rate, 20.45%) with the use of six RS variables as predictors. The four-type (see Supplementary Table S1[1]) and six-type (see Supplementary Table S2[1]) partitions presented accuracies of 75% and 71.45%, respectively, and neither of them selected

[1]Supplementary data are available with the article through the journal Web site at http://nrcresearchpress.com/doi/suppl/10.1139/cjfr-2014-0430.

less than six RS variables as predictors. Therefore, the five-type partition was selected as the basis for representing the regeneration types (Table 1). The characteristics of the five regeneration types were as follows: type 1, characterized by a very low vegetation cover; type 2, characterized by very low tree regeneration but remarkable shrubs abundance; type 3, included hardwoods in low to moderate cover mixed with shrubs; type 4, presented high cover of hardwood regeneration; type 5, consisting of stands dominated by pine regeneration in moderate to high cover (Table 1; Fig. 3).

The following six RS variables were selected to identify the five regeneration types: the 10th and 95th percentile height (H_P10 and H_P95, respectively), the percentage of first returns above the mode of the height distribution (H_abMODE), the coefficient of variation of the height distribution (H_CV), the 1st quartile NDVI (NDVI_Q1), and the percentage of plot with NDVI between 0.15 and 0.3 (NDVI_15_30) (Fig. 4). OOB classification accuracies of the RF model by regeneration type were 80% for type 1, 100% for type 2, 81.8% for type 3, 70% for type 4, and 76.9% for type 5.

Mapping postfire regeneration types and validation with visual estimates

The whole study area (3191.8 ha) was classified into the five regeneration types (Fig. 5). More than a decade after the wildfire, almost one-half of the area (42.6%) showed high tree cover, with a clear dominance of resprouting hardwoods (type 4). About 17% of the study area was still dominated by resprouting hardwoods but with low to moderate tree cover (type 3). Pine regeneration appeared in moderate to high cover in approximately 11% of the study area. Finally, the rest of the area showed sparse or no tree regeneration (type 2 and type 1, respectively) (Table 2). Patches of type 1 and type 3 were usually very small (i.e., with an area smaller than 0.1 ha), with type 1 showing the most regular patch shape (i.e., closer to a circular shape). In contrast, type 4 had the highest amount of area covered by large patches (0.1–1 ha, 1–5 ha, and >5 ha) and showed the most irregular shapes. Type 2 and type 5 were also present in a wide range of patch sizes, but in them, small patches were more common than in type 4.

The evaluation of classification accuracy compared with visual estimation resulted in 82.7% accurately classified plots (between 74.1% and 91.2% were accurately classified with a 95% confidence interval), being close to the OOB classification accuracy obtained for the training dataset. Type 1 and type 5 showed the highest classification accuracy, at 93.3% (95% confidence interval, 80.7%–100%) and approximately 92.3% (77.8%–100%), respectively. The classification of type 4 was also highly accurate, with 84.6% (65%–100%) of plots accurately classified. Finally, type 2 (shrub dominance with very low tree cover) and type 3 (low to moderate tree cover dominated by hardwoods) reported lower classification accuracies, with 72.2% (51.5%–92.9%) and 75% (53.8%–96.2%) of plots accurately classified, respectively.

Discussion

This study presents a methodological approach that combines airborne LiDAR data and single-date NDVI data, computed from aerial images, to provide precise, georeferenced, and spatially continuous information on postfire regeneration over a large area. The presented methodology was not intended for short-term assessments — for which, the analysis of NDVI values extracted from satellite imagery may be enough (Diaz-Delgado et al. 2003; Gouveia et al. 2010; van Leeuwen et al. 2010; Vicente-Serrano et al. 2011; Vila and Barbosa 2010) — but for mid- to long-term assessments, which are crucial for appropriately designing and planning postdisturbance silvicultural treatments (Alloza and Vallejo 2006; Bauhus et al. 2013; Stephens et al. 2010). The information generated by this methodology provides forest stand structure and composition information that can be used to predict its potential evolution patterns, detect areas with persistent regeneration problems, and delimit forest stands for planning management operations. This ultimately enables management interventions to be prioritized and allocated.

Fig. 4. Variable importance plot for the for the five-type classification model of postfire regeneration types. Higher values of mean decrease accuracy represent higher variable importance in the model. See Materials and methods for variable definitions.

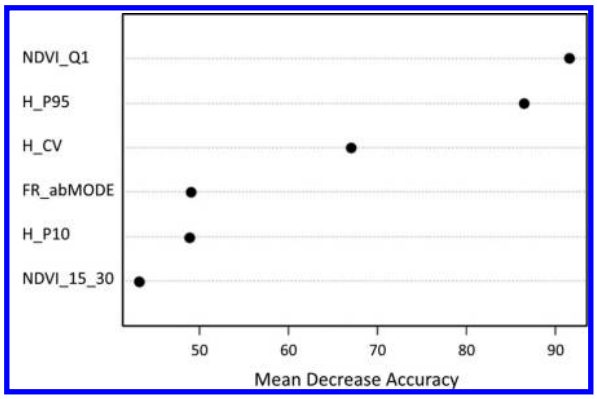

There are some differences between our RS-based assessment and evaluations traditionally made from field-based inventories. On one hand, the level of detail in describing the postfire vegetation communities is, in general, higher in field-based inventories where measurements are conducted at individual-plant level (e.g., Curt et al. 2009; Proença et al. 2010). However, RS-based assessments entail less time and fewer spatial constraints than field inventories, as they are much less time consuming and less exposed to the uncertainties associated with inference and estimation from sample surveys in areas showing fine-scale heterogeneity. Assessments based on RS data also allow for the estimation of quantitative tree and forest attributes across large areas by using regression methods (e.g., Andersen et al. 2005; García et al. 2010; Latifi et al. 2012; Wulder et al. 2009). However, that approach requires working with high-resolution LiDAR data, especially when forest attributes are related to low vegetation. In our case, we aggregated RS metrics to the plot level (10 m × 10 m) to make a community-based assessment instead of a plant-based assessment, and we estimated forest types instead of quantitative forest attributes, in concordance with the potential and limitations of the available low-resolution LiDAR data. Our approach permits the discernment between regeneration types by using height and intensity variables from LiDAR data and NDVI metrics, computed from single-date multispectral aerial imagery, thus providing forest managers with most of the information that they need for midterm operational planning of restoration activities and silvicultural operations (Vallejo et al. 2012). In addition, the provision of continuous, spatially explicit information at the landscape scale allows for easy implementation of relevant forestry applications such as the characterization and mapping of forest canopy fuels and fire risk (Erdody and Moskal 2010; García et al. 2011; González-Olabarria et al. 2012; Mutlu et al. 2008; Pierce et al. 2012; Riaño et al. 2007). The resulting maps of regeneration types also offer a starting point for the analysis of postdisturbance vegetation dynamics at large scales (Debouk et al. 2013; Goetz et al. 2010; Holmgren et al. 2008). Our methodology is appropriate for large-scale assessment, as regional and national LiDAR coverages are often collected at low resolutions. The NDVI data that we used were derived from four-band aerial imagery, which are being used more and more frequently for national surveys. They have higher spatial resolution that the data derived from satellite imagery, although they are more limited for multitemporal analyses due to the generally low temporal resolution.

Our approach requires a prior categorization of the vegetation that is to be extrapolated using RS data. Such characterization can

Fig. 5. Spatial distribution of regeneration types in the study area.

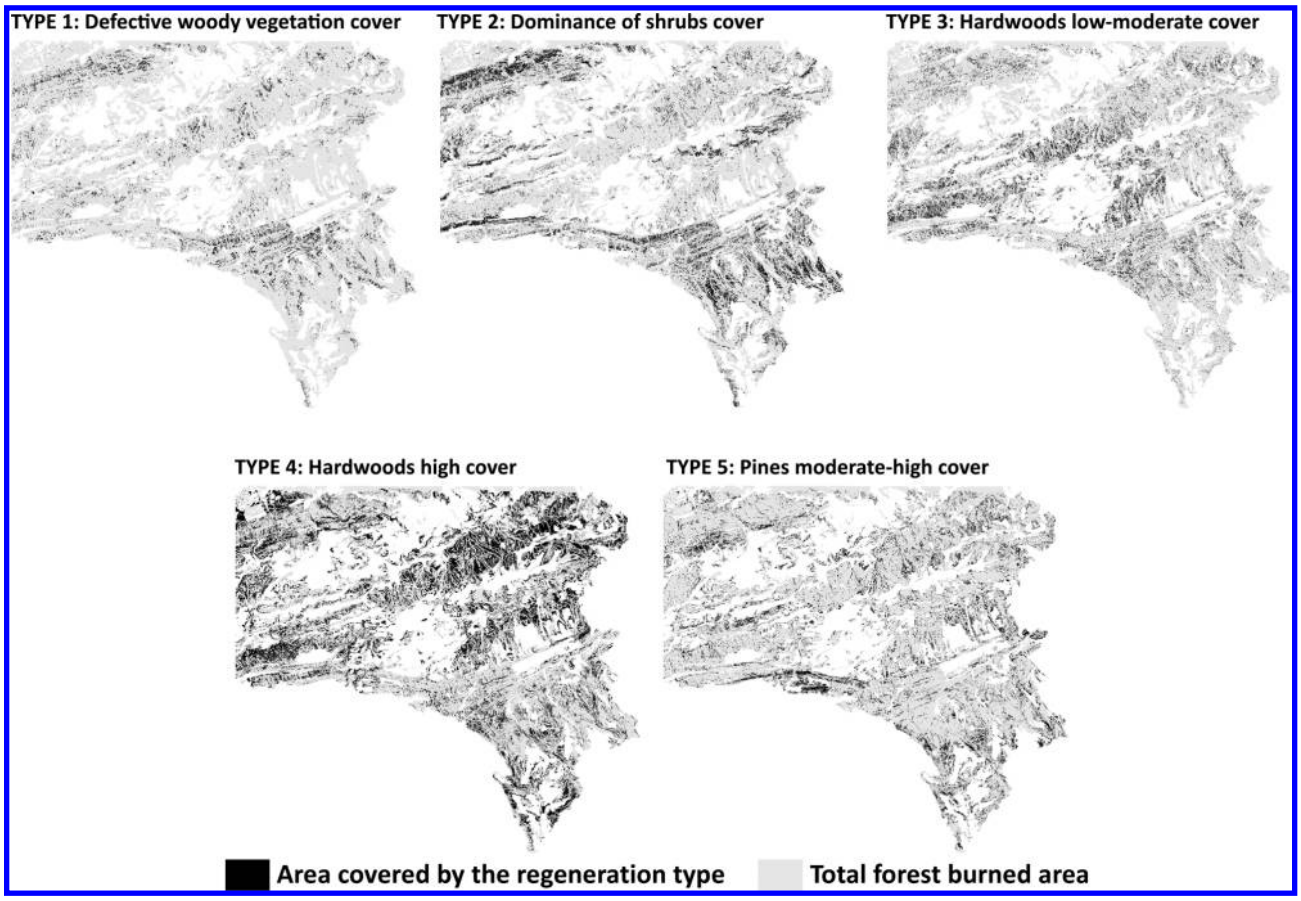

Table 2. Basic patch size and shape characterization of the five regeneration types in the study area.

			% of TYPE area by size classes						
Type	Area (ha)	Area (% of total)	<0.1 ha	0.1–1 ha	1–5 ha	>5 ha	PS_m (ha)	PS_{cv} (%)	MSI
1	298.3	9.35	79.16	20.84	0.00	0.00			
2	652.0	20.43	57.67	28.13	12.17	2.03	0.0177	83.1	1.232
3	532.3	16.68	80.26	19.55	0.20	0.00	0.0169	82.1	1.203
4	1359.0	42.58	32.63	36.32	25.15	5.90	0.0198	86.1	1.291
5	350.2	10.97	59.96	30.04	7.76	2.23	0.0177	85.0	1.223

Note: Total area was 3191.8 ha. PS_m, patch size mean; PS_{cv}, patch size coefficient of variation; MSI, mean shape index.

be achieved not only by generating vegetation typologies from the analysis of quantitative field data (as presented here), but also by using existing classifications when types of vegetation are previously known (Falkowski et al. 2009). Other areas may have different prefire forest composition and structure or be more or less severely impacted by fire and present different postfire regeneration trajectories. Thus the number and characteristics of the regeneration types may change from one area to the other, and the RS variables selected for the classification model will be different in each particular case, as other types of vegetation may be better explained by a different combination of RS variables. In our case, the best fit was attained with just a combination of LiDAR height and NDVI variables. LiDAR-normalized intensity variables were not found to be essential in discerning our regeneration types, but they could be more important in other cases (Bork and Su 2007; Donoghue et al. 2007; García et al. 2010).

Our methodology is applicable as long as the input data (LiDAR and NDVI) are available and the chosen typologies can be accurately reproduced using supervised classification of RS data. Even so, to exploit the full potential of combining LiDAR and NDVI data for vegetation characterization, our approach calls for a certain period of time to pass between the occurrence of the disturbance and the acquisition of the RS data to allow for height differentiation between species and groups of species. Other aspects that must be considered when applying this methodology are the characteristics of the RS data available, particularly in terms of collection dates (year and season) and spatial resolution. In this regard, increasing the intensity of field sampling would be necessary for a disturbed area for which date and season of collection of the RS data are not comparable. Meanwhile, the spatial resolution of the RS data available may dictate how the level of detail in characterizing regeneration types needs to be adapted. Finally, the use of this methodology also requires good knowledge of the vegetation in the specific area under study and a decision about the desired level of detail when categorizing it to adequately design the field inventory, with more heterogeneous environments typically requiring a denser network of field plots.

The five regeneration types obtained in our study area adequately represent the wide range of postfire conditions described in previous field studies (Retana et al. 2002, 2012; Rodrigo et al. 2004). Furthermore, the results of the field validation revealed high (>80%) overall classification accuracy levels. For three of the

five types, the field validation matched the classification implemented through RS variables in >80% of the cases. The types dominated by shrubs with very low tree cover (i.e., type 2) and by low to moderate tree cover dominated by hardwoods (i.e., type 3) showed sensibly lower accuracy levels (around 70%–75%). Most of the misclassified type 2 plots were assigned to type 3, meaning that the cover of hardwoods was overestimated in the classification model based on RS data. Misclassified type 3 plots were assigned to type 4 (very similar to type 3, as they are dominated by hardwoods regeneration but with higher hardwoods cover). Overall, misclassification problems could be considered relatively small and occurred among closely related regeneration types. Interestingly, two of the regeneration types of major interest for management purposes (type 1, with defective cover of woody vegetation, and type 5, with moderate to high tree cover of pine regeneration) were identified with high accuracy. In the case of type 5, this may indicate very good performance of NDVI-derived variables for species differentiation, as previously shown in other studies (Hill et al. 2010; Key et al. 2001).

Regarding the spatial distribution of the forest regeneration, we found resprouting hardwoods to be presently dominating almost 60% of the area that was formerly dominated by pines. These results demonstrate the important species-dominance shifts that crown fires may induce in Mediterranean black pine forests, as reported by Rodrigo et al. (2004). However, it should be stressed that the level of detail achieved in our study did not allow for proper identification of the presence of small pines on forest areas that were dominated by high shrubs or hardwoods, leading to certain underestimation of the pine regeneration. Interestingly, we also found <10% of the burned area to be in high risk of soil erosion due to a defective cover of woody vegetation. This lack of regeneration appeared in very small patches, which sometimes could be associated with the presence of small rocky outcrops.

The information generated through our methodological approach should be useful for the definition of vegetation management and restoration strategies over large areas affected by disturbances, as it helps to identify areas where woody species are struggling to regenerate (thus potentially needing restoral actions) and to provide information on areas showing regeneration success and their current vegetation structure. For example, restoration actions designed to facilitate tree cover recovery could be envisaged areas of our case study where the predominant postfire regeneration pattern was identified as type 1 and type 2, especially in the larger patches (more frequently classed as type 2). In parallel, early thinning interventions designed to reduce competition, increase tree growth and vigor, and reduce the amount and continuity of fuels could be planned for patches classified as type 5 (Gonzalez-Olabarria et al. 2008; Moya et al. 2008; Verkaik and Espelta 2006), whereas coppice thinning could be proposed for stands classified as type 4 (Cotillas et al. 2009; Espelta et al. 2003*b*; Sanchez-Humanes and Espelta 2011).

Acknowledgements

This research was primarily supported by the Spanish Ministry of Science and Innovation via the RESILFOR project (AGL2012-40039-C02-01). It also was part of a cooperative agreement between the Forest Sciences Center of Catalonia and the Institut Cartogràfic i Geològic de Catalunya aimed at using aerial RS data for forest characterization. The Catalan Agency for Management of University and Research Grants provided S.M.A. with support through a "predoctoral" grant (FI-DGR), and the Spanish Ministry of Science and Innovation provided L.C., J.R.G., and M.C. with support through postdoctoral "Ramon y Cajal" contracts. Finally, the authors are very grateful to Vicent Vidal, Sergio Martinez, and Assu Gil for their invaluable help in the collection of the field data.

References

Alloza, J.A., and Vallejo, R. 2006. Restoration of burned areas in forest management plans. *In* Desertification in the Mediterranean region. A security issue. *Edited by* W. Kepner, J. Rubio, D. Mouat, and F. Pedrazzini. Springer Netherlands. pp. 475–488.

Andersen, H.-E., McGaughey, R.J., and Reutebuch, S.E. 2005. Estimating forest canopy fuel parameters using LIDAR data. Remote Sens. Environ. **94**(4): 441–449. doi:10.1016/j.rse.2004.10.013.

Aubury, S., Bruciamacchie, M., and Druelle, P. 1990. L'inventaire typologique : un outil performant pour l'elaboration des amenagements ou plans simples de gestion. Rev. For. Fr. (4): 429–444. doi:10.4267/2042/26090.

Bauhus, J., Puettmann, K.J., and Kühne, C. 2013. Close-to-nature forest management in Europe. *In* Managing forests as complex adaptive systems: building resilience to the challenge of global change. *Edited by* C. Messier, K.J. Puettmann, and K.D. Coates. The Earthscan Forest Library, New York.

Belda, F., and Meliá, J. 2000. Relationships between climatic parameters and forest vegetation: application to burned area in Alicante (Spain). Forest. Ecol. Manage. **135**(1–3): 195–204. doi:10.1016/S0378-1127(00)00310-8.

Bork, E.W., and Su, J.G. 2007. Integrating LIDAR data and multispectral imagery for enhanced classification of rangeland vegetation: a meta analysis. Remote Sens. Environ. **111**(1): 11–24. doi:10.1016/j.rse.2007.03.011.

Breiman, L. 2001. Random forests. Machine Learning, **45**(1): 5–32. doi:10.1023/A:1010933404324.

Burriel, J.A., Gracia, C., Ibàñez, J.J., Mata, T., and Vayreda, J. 2004. Inventari Ecològic i Forestal de Catalunya. CREAF, Bellaterra, Barcelona, Spain.

Carrión, J.S., Fernández, S., González-Sampériz, P., Gil-Romera, G., Badal, E., Carrión-Marco, Y., López-Merino, L., López-Sáez, J.A., Fierro, E., and Burjachs, F. 2010. Expected trends and surprises in the late glacial and Holocene vegetation history of the Iberian Peninsula and Balearic Islands. Rev. Palaeobot. Palynol. **162**(3): 458–475. doi:10.1016/j.revpalbo.2009.12.007.

Coren, F., and Sterzai, P. 2006. Radiometric correction in laser scanning. Int. J. Remote Sens. **27**(15): 3097–3104. doi:10.1080/01431160500217277.

Cotillas, M., Sabaté, S., Gracia, C., and Espelta, J.M. 2009. Growth response of mixed mediterranean oak coppices to rainfall reduction. Could selective thinning have any influence on it? For. Ecol. Manage. **258**(7): 1677–1683. doi:10.1016/j.foreco.2009.07.033.

Centre for Ecological Research and Forestry Applications (CREAF). 1993. Mapa de cobertes del sòl de Catalunya v1. *Edited by* D.d.A. Centre de Recerca Ecològica i Aplicacions Forestals, Ramaderia, Pesca, Alimentació i Medi Natural, Interior i Territori i Sostenibilitat. Generalitat de Catalunya. [In Spanish.]

Cubo María, J.E., Enríquez Alcalde, E., Gallar Pérez-Pastor, J.J., Jemes Díaz, V., López García, M., Mateo Díez, M.L., Muñoz Correal, A., and Parra Orgaz, P.J. 2012. Los incendios forestales en España. Decenio 2001–2010. [In Spanish.]

Curt, T., Adra, W., and Borgniet, L. 2009. Fire-driven oak regeneration in French Mediterranean ecosystems. For. Ecol. Manage. **258**(9): 2127–2135. doi:10.1016/j.foreco.2009.08.010.

Cutler, D.R., Edwards, T.C., Beard, K.H., Cutler, A., Hess, K.T., Gibson, J., and Lawler, J.J. 2007. Random forests for classification in ecology. Ecology, **88**(11): 2783–2792. doi:10.1890/07-0539.1.

Debouk, H., Riera-Tatché, R., and Vega-García, C. 2013. Assessing post-fire regeneration in a Mediterranean mixed forest using lidar data and artificial neural networks. Photogramm. Eng. Remote Sens. **79**(12): 1121–1130. doi:10.14358/PERS.79.12.1121.

Dirección General de Conservación de la Naturaleza (DGCN). 2001. Mapa Forestal de España. Escala 1:50.000. Cataluña. Organismo Autónomo de Parques Nacionales (MMA), Madrid, Spain.

Diaz-Delgado, R., Llorett, F., and Pons, X. 2003. Influence of fire severity on plant regeneration by means of remote sensing imagery. Int. J. Remote Sens. **24**(8): 1751–1763. doi:10.1080/01431160210144732.

Donoghue, D.N.M., Watt, P.J., Cox, N.J., and Wilson, J. 2007. Remote sensing of species mixtures in conifer plantations using LiDAR height and intensity data. Remote Sens. Environ. **110**(4): 509–522. doi:10.1016/j.rse.2007.02.032.

European Forest Institute (EFI). 2010. A Mediterranean forest research agenda (2010–2020) — MFRA. Available from http://www.efimed.efi.int/files/attachments/efimed/mediterranean_forest_research_agenda_2010-2020.pdf [accessed May 2014].

Elmqvist, T., Folke, C., Nystrom, M., Peterson, G., Bengtsson, J., Walker, B., and Norberg, J. 2003. Response diversity, ecosystem change, and resilience. Front. Ecol. Environ. **1**(9): 488–494. doi:10.1890/1540-9295(2003)001[0488:RDECAR]2.0.CO;2.

Erdody, T.L., and Moskal, L.M. 2010. Fusion of LiDAR and imagery for estimating forest canopy fuels. Remote Sens. Environ. **114**(4): 725–737. doi:10.1016/j.rse.2009.11.002.

Espelta, J.M., Retana, J., and Habrouk, A. 2003*a*. An economic and ecological multi-criteria evaluation of reforestation methods to recover burned *Pinus nigra* forests in NE Spain. For. Ecol. Manage. **180**(1–3): 185–198. doi:10.1016/S0378-1127(02)00599-6.

Espelta, J.M., Retana, J., and Habrouk, A. 2003*b*. Resprouting patterns after fire and response to stool cleaning of two coexisting Mediterranean oaks with contrasting leaf habits on two different sites. For. Ecol. Manage. **179**(1–3): 401–414. doi:10.1016/S0378-1127(02)00541-8.

Evans, J.S., and Cushman, S.A. 2009. Gradient modeling of conifer species using random forests. Landsc. Ecol. **24**(5): 673–683. doi:10.1007/s10980-009-9341-0.

Evans, J., Murphy, M., Holden, Z., and Cushman, S. 2011. Modeling species distribution and change using random forest. *In* Predictive species and habitat modeling in landscape ecology. *Edited by* C.A. Drew, Y.F. Wiersma, and F. Huettmann. Springer New York. pp. 139–159.

Falkowski, M.J., Evans, J.S., Martinuzzi, S., Gessler, P.E., and Hudak, A.T. 2009. Characterizing forest succession with lidar data: an evaluation for the Inland Northwest, U.S.A. Remote Sens. Environ. **113**(5): 946–956. doi:10.1016/j.rse.2009.01.003.

García, M., Riaño, D., Chuvieco, E., and Danson, F.M. 2010. Estimating biomass carbon stocks for a Mediterranean forest in central Spain using LiDAR height and intensity data. Remote Sens. Environ. **114**(4): 816–830. doi:10.1016/j.rse.2009.11.021.

García, M., Riaño, D., Chuvieco, E., Salas, J., and Danson, F.M. 2011. Multispectral and LiDAR data fusion for fuel type mapping using support vector machine and decision rules. Remote Sens. Environ. **115**(6): 1369–1379. doi:10.1016/j.rse.2011.01.017.

Goetz, S.J., Sun, M., Baccini, A., and Beck, P.S.A. 2010. Synergistic use of spaceborne lidar and optical imagery for assessing forest disturbance: an Alaska case study. J. Geophys. Res. Biogeogr. **115**(G2): G00E07. doi:10.1029/2008JG000898.

Gonzalez-Olabarria, J.R., and Pukkala, T. 2007. Characterization of forest fires in Catalonia (north–east Spain). Eur. J. For. Res. **126**(3): 421–429. doi:10.1007/s10342-006-0164-0.

Gonzalez-Olabarria, J.R., Palahi, M., Pukkala, T., and Trasobares, A. 2008. Optimising the management of *Pinus nigra* Arn. stands under endogenous risk of fire in Catalonia. Inv. Agrar: Sist. Recursos Fores. **17**(1): 10–17. doi:10.5424/srf/2008171-01019.

González-Olabarria, J.-R., Rodríguez, F., Fernández-Landa, A., and Mola-Yudego, B. 2012. Mapping fire risk in the model forest of Urbión (Spain) based on airborne LiDAR measurements. For. Ecol. Manage. **282**: 149–156. doi:10.1016/j.foreco.2012.06.056.

Gouveia, C., DaCamara, C.C., and Trigo, R.M. 2010. Post-fire vegetation recovery in Portugal based on spot/vegetation data. Nat. Hazard. Earth Sys. **10**(4): 673–684. doi:10.5194/nhess-10-673-2010.

Hair, J.F., Tatham, R.L., Anderson, R.E., and Black, W. 2009. Multivariate data analysis. 7th edition. Pearson.

Herbert, I., and Rebeirot, F. 1985. Les futaies jardinées du Haut-Jura. Rev. For. Fr. **XXXVII**(6): 465–481.

Hill, R.A., Wilson, A.K., George, M., and Hinsley, S.A. 2010. Mapping tree species in temperate deciduous woodland using time-series multi-spectral data. Appl. Veg. Sci. **13**(1): 86–99. doi:10.1111/j.1654-109X.2009.01053.x.

Holmgren, J., Persson, Å., and Söderman, U. 2008. Species identification of individual trees by combining high resolution LiDAR data with multi-spectral images. Int. J. Remote Sens. **29**(5): 1537–1552. doi:10.1080/01431160701736471.

Hudak, A.T., Strand, E.K., Vierling, L.A., Byrne, J.C., Eitel, J.U.H., Martinuzzi, S., and Falkowski, M.J. 2012. Quantifying aboveground forest carbon pools and fluxes from repeat LiDAR surveys. Remote Sens. Environ. **123**: 25–40. doi:10.1016/j.rse.2012.02.023.

Johnstone, J.F., Chapin, F.S., III, Foote, J., Kemmett, S., Price, K., and Viereck, L. 2004. Decadal observations of tree regeneration following fire in boreal forests. Can. J. For. Res. **34**(2): 267–273. doi:10.1139/x03-183.

Keenan, T., Maria, Serra, J., Lloret, F., Ninyerola, M., and Sabate, S. 2011. Predicting the future of forests in the Mediterranean under climate change, with niche- and process-based models: CO_2 matters! Glob. Chang. Biol. **17**(1): 565–579. doi:10.1111/j.1365-2486.2010.02254.x.

Key, T., Warner, T.A., McGraw, J.B., and Fajvan, M.A. 2001. A Comparison of multispectral and multitemporal information in high spatial resolution imagery for classification of individual tree species in a temperate hardwood forest. Remote Sens. Environ. **75**(1): 100–112. doi:10.1016/S0034-4257(00)00159-0.

Kornus, W., and Ruiz, A. 2003. Strip adjustment of LIDAR data. 3-D reconstruction from Airborne Laserscanner and InSAR Data, **34**(3): 47–50.

Kukko, A., Kaasalainen, S., and Litkey, P. 2008. Effect of incidence angle on laser scanner intensity and surface data. Appl. Opt. **47**(7): 986–992. doi:10.1364/AO.47.000986.

Latifi, H., Fassnacht, F., and Koch, B. 2012. Forest structure modeling with combined airborne hyperspectral and LiDAR data. Remote Sens. Environ. **121**(0): 10–25. doi:10.1016/j.rse.2012.01.015.

Lefsky, M.A., Cohen, W.B., Parker, G.G., and Harding, D.J. 2002. Lidar remote sensing for ecosystem studies. Bioscience, **52**(1): 19–30. doi:10.1641/0006-3568(2002)052[0019:LRSFES]2.0.CO;2.

Liaw, A., and Wiener, M. 2002. Classification and regression by randomForest. R News, **2**(3): 18–22.

Lindner, M., Maroschek, M., Netherer, S., Kremer, A., Barbati, A., Garcia-Gonzalo, J., Seidl, R., Delzon, S., Corona, P., Kolstrom, M., Lexer, M.J., and Marchetti, M. 2010. Climate change impacts, adaptive capacity, and vulnerability of European forest ecosystems. For. Ecol. Manage. **259**(4): 698–709. doi:10.1016/j.foreco.2009.09.023.

Loepfe, L., Martinez-Vilalta, J., Oliveres, J., Piñol, J., and Lloret, F. 2010. Feedbacks between fuel reduction and landscape homogenisation determine fire regimes in three Mediterranean areas. For. Ecol. Manage. **259**(12): 2366–2374. doi:10.1016/j.foreco.2010.03.009.

Martin-Alcon, S., Coll, L., and Aunos, A. 2012. A broad-scale analysis of the main factors determining the current structure and understory composition of Catalonian sub-alpine (*Pinus uncinata* Ram.) forests. Forestry, **85**(2): 225–236. doi:10.1093/forestry/cpr067.

Martínez, L., Pérez, F., Arbiol, R., and Magariños, A. 2012. Development of NDVI WMS geoservice from reflectance DMC imagery at ICC. *In* International Calibration and Orientation Workshop EuroCOW 2012, Castelldefels, Barcelona, Spain.

McGaughey, R.J., and Carson, W.W. 2003. Fusing LIDAR data, photographs, and other data using 2D and 3D visualization techniques. *In* Terrain data: applications and visualization — making the connection. Charleston, South Carolina; Bethesda, Maryland. American Society for Photogrammetry and Remote Sensing. pp. 16–24.

Morsdorf, F., Kötz, B., Meier, E., Itten, K.I., and Allgöwer, B. 2006. Estimation of LAI and fractional cover from small footprint airborne laser scanning data based on gap fraction. Remote Sens. Environ. **104**(1): 50–61. doi:10.1016/j.rse.2006.04.019.

Moya, D., Heras, J.D.L., Lopez-Serrano, F.R., and Leone, V. 2008. Optimal intensity and age of management in young Aleppo pine stands for post-fire resilience. For. Ecol. Manage. **255**(8–9): 3270–3280. doi:10.1016/j.foreco.2008.01.067.

Mutlu, M., Popescu, S.C., Stripling, C., and Spencer, T. 2008. Mapping surface fuel models using lidar and multispectral data fusion for fire behavior. Remote Sens. Environ. **112**(1): 274–285. doi:10.1016/j.rse.2007.05.005.

Niinemets, U., and Valladares, F. 2006. Tolerance to shade, drought, and waterlogging of temperate Northern Hemisphere trees and shrubs. Ecological Monographs, **76**(4): 521–547. doi:10.1890/0012-9615(2006)076.

Ordoñez, J.L., and Retana, J. 2004. Early reduction of post-fire recruitment of *Pinus nigra* by post-dispersal seed predation in different time-since-fire habitats. Ecography, **27**(4): 449–458. doi:10.1111/j.0906-7590.2004.03886.x.

Ordoñez, J.L., LAST NAME, XX, and LAST NAME, XX 2005. NAME OF ARTICLE. JOURNAL, **VOLUME**: PAGE RANGE. DOI.

Pausas, J.G., Ribeiro, E., and Vallejo, R. 2004. Post-fire regeneration variability of *Pinus halepensis* in the eastern Iberian Peninsula. For. Ecol. Manage. **203**(1–3): 251–259. doi:10.1016/j.foreco.2004.07.061.

Pausas, J.C., Llovet, J., Rodrigo, A., and Vallejo, R. 2008. Are wildfires a disaster in the Mediterranean basin? — a review. Int. J. Wildland Fire, **17**(6): 713–723. doi:10.1071/WF07151.

Pierce, A.D., Farris, C.A., and Taylor, A.H. 2012. Use of random forests for modeling and mapping forest canopy fuels for fire behavior analysis in Lassen Volcanic National Park, California, U.S.A. For. Ecol. Manage. **279**(0): 77–89. doi:10.1016/j.foreco.2012.05.010.

Piñol, J., Terradas, J., and Lloret, F. 1998. Climate warming, wildfire hazard, and wildfire occurrence in coastal eastern Spain. Clim. Change, **38**(3): 345–357. doi:10.1023/A:1005316632105.

Proença, V., Pereira, H.M., and Vicente, L. 2010. Resistance to wildfire and early regeneration in natural broadleaved forest and pine plantation. Acta Oecol. **36**(6): 626–633. doi:10.1016/j.actao.2010.09.008.

Puerta-Piñero, C., Brotons, L., Coll, L., and González-Olabarría, J.R. 2011. Valuing acorn dispersal and resprouting capacity ecological functions to ensure Mediterranean forest resilience after fire. Eur. J. For. Res. **131**(3): 835–844. doi:10.1007/s10342-011-0557-6.

Puerta-Piñero, C., Espelta, J.M., Sánchez-Humanes, B., Rodrigo, A., Coll, L., and Brotons, L. 2012. History matters: previous land use changes determine post-fire vegetation recovery in forested Mediterranean landscapes. For. Ecol. Manage. **279**: 121–127. doi:10.1016/j.foreco.2012.05.020.

R Development Core Team. 2007. R: a language and environment for statistical computing.

Rempel, R.S., Kaukinen, D., and Carr, A.P. 2012. Patch analyst and patch grid. *Edited by* Ontario Ministry of Natural Resources and Forestry. Centre for Northern Forest Ecosystem Research, Thunder Bay, Ontario.

Reque, J.A., and Bravo, F. 2008. Identifying forest structure types using national forest inventory data: the case of sessile oak forest in the Cantabrian range. Inv. Agrar: Sist. Recursos Fores. **17**(2): 105–113. doi:10.5424/srf/2008172-01027.

Resco de Dios, V., Fischer, C., and Colinas, C. 2006. Climate change effects on Mediterranean forests and preventive measures. New For. **33**(1): 29–40. doi:10.1007/s11056-006-9011-x.

Retana, J., Espelta, J.M., Habrouk, A., Ordonez, J.L., and de Sola-Morales, F. 2002. Regeneration patterns of three Mediterranean pines and forest changes after a large wildfire in northeastern Spain. Ecoscience, **9**(1): 89–97.

Retana, J., Arnan, X., Arianoutsou, M., Barbati, A., Kazanis, D., and Rodrigo, A. 2012. Post-fire management of non-serotinous pine forests. *In* Post-fire management and restoration of southern European forests. *Edited by* F. Moreira, M. Arianoutsou, P. Corona, and J. De las Heras. Springer Netherlands. pp. 151–170.

Riaño, D., Chuvieco, E., Ustin, S., Zomer, R., Dennison, P., Roberts, D., and Salas, J. 2002. Assessment of vegetation regeneration after fire through multitemporal analysis of AVIRIS images in the Santa Monica Mountains. Remote Sens. Environ. **79**(1): 60–71. doi:10.1016/S0034-4257(01)00239-5.

Riaño, D., Chuvieco, E., Ustin, S.L., Salas, J., Rodríguez-Pérez, J.R., Ribeiro, L.M., Viegas, D.X., Moreno, J.M., and Fernández, H. 2007. Estimation of shrub height for fuel-type mapping combining airborne LiDAR and simultaneous color infrared ortho imaging. Int. J. Wildland Fire, **16**(3): 341–348. doi:10.1071/WF06003.

Rodrigo, A., Retana, J., and Picó, F.X. 2004. Direct regeneration is not the only

response of Mediterranean forests to large fires. Ecology, **85**(3): 716–729. doi:10.1890/02-0492.

Roman-Cuesta, R.M., Gracia, M., and Retana, J. 2009. Factors influencing the formation of unburned forest islands within the perimeter of a large forest fire. Forest. Ecol. Manag. **258**(2): 71–80. doi:10.1016/j.foreco.2009.03.041.

Sanchez-Humanes, B., and Espelta, J.M. 2011. Increased drought reduces acorn production in *Quercus ilex* coppices: thinning mitigates this effect but only in the short term. Forestry, **84**(1): 73–82. doi:10.1093/forestry/cpq045.

San-Miguel-Ayanz, J., Schulte, E., Schmuck, G., and Camia, A. 2013. The European forest fire information system in the context of environmental policies of the European Union. Forest Policy and Economics, **29**(0): 19–25. doi:10.1016/j.forpol.2011.08.012.

Schelhaas, M.J., Nabuurs, G.J., and Schuck, A. 2003. Natural disturbances in the European forests in the 19th and 20th centuries. Glob. Chang. Biol. **9**(11): 1620–1633. doi:10.1046/j.1365-2486.2003.00684.x.

Selkimäki, M., González-Olabarria, J.R., and Pukkala, T. 2012. Site and stand characteristics related to surface erosion occurrence in forests of Catalonia (Spain). Eur. J. For. Res. **131** (3): 727–738. doi:10.1007/s10342-011-0545-x.

Shatford, J.P.A., Hibbs, D.E., and Puettmann, K.J. 2007. Conifer regeneration after forest fire in the Klamath–Siskiyous: how much, how soon? J. For. **105**(3): 139–146.

Stephens, S.L., Millar, C.I., and Collins, B.M. 2010. Operational approaches to managing forests of the future in Mediterranean regions within a context of changing climates. Environ. Res. Lett. **5**(2): 1–9. doi:10.1088/1748-9326/5/2/024003.

Terrasolid. 2012. TerraScan user's suide. Terrasolid, Helsinki, Finland.

Tucker, C.J. 1979. Red and photographic infrared linear combinations for monitoring vegetation. Remote Sens. Environ. **8**(2): 127–150. doi:10.1016/0034-4257(79)90013-0.

Vallejo, V.R., Arianoutsou, M., and Moreira, F. 2012. Fire ecology and post-fire restoration approaches in southern European forest types. *In* Post-fire management and restoration of southern European forests. *Edited by* F. Moreira, M. Arianoutsou, P. Corona, and J. De las Heras. Springer Netherlands. pp. 93–119.

van Leeuwen, W.J.D., Casady, G.M., Neary, D.G., Bautista, S., Alloza, J.A., Carmel, Y., Wittenberg, L., Malkinson, D., and Orr, B.J. 2010. Monitoring post-wildfire vegetation response with remotely sensed time-series data in Spain, U.S.A. and Israel. Int. J. Wildland Fire, **19**(1): 75–93. doi:10.1071/WF08078.

Verkaik, I., and Espelta, J.M. 2006. Post-fire regeneration thinning, cone production, serotiny and regeneration age in *Pinus halepensis*. For. Ecol. Manage. **231**(1–3): 155–163. doi:10.1016/j.foreco.2006.05.041.

Vicente-Serrano, S.M., Pérez-Cabello, F., and Lasanta, T. 2011. *Pinus halepensis* regeneration after a wildfire in a semiarid environment: assessment using multitemporal Landsat images. Int. J. Wildland Fire, **20**(2): 195–208. doi:10.1071/WF08203.

Viedma, O., Meliá, J., Segarra, D., and Garcia-Haro, J. 1997. Modeling rates of ecosystem recovery after fires by using landsat TM data. Remote Sens. Environ. **61**(3): 383–398. doi:10.1016/S0034-4257(97)00048-5.

Vila, J.P.S., and Barbosa, P. 2010. Post-fire vegetation regrowth detection in the Deiva Marina region (Liguria–Italy) using Landsat TM and ETM plus data. Ecol. Model. **221**(1): 75–84. doi:10.1016/j.ecolmodel.2009.03.011.

Vilà-Cabrera, A., Rodrigo, A., Martínez-Vilalta, J., and Retana, J. 2012. Lack of regeneration and climatic vulnerability to fire of Scots pine may induce vegetation shifts at the southern edge of its distribution. J. Biogeogr. **39**(3): 488–496. doi:10.1111/j.1365-2699.2011.02615.x.

Ward, J.H., Jr. 1963. Hierarchical grouping to optimize an objective function. J. Am. Stat. Assoc. **58**: 236–244. doi:10.2307/2282967.

Waser, L.T., Ginzler, C., Kuechler, M., Baltsavias, E., and Hurni, L. 2011. Semi-automatic classification of tree species in different forest ecosystems by spectral and geometric variables derived from airborne digital sensor (ADS40) and RC30 data. Remote Sens. Environ. **115**(1): 76–85. doi:10.1016/j.rse.2010.08.006.

Wulder, M.A., White, J.C., Alvarez, F., Han, T., Rogan, J., and Hawkes, B. 2009. Characterizing boreal forest wildfire with multi-temporal Landsat and LIDAR data. Remote Sens. Environ. **113**(7): 1540–1555. doi:10.1016/j.rse.2009.03.004.

Wulder, M.A., White, J.C., Nelson, R.F., Næsset, E., Ørka, H.O., Coops, N.C., Hilker, T., Bater, C.W., and Gobakken, T. 2012. Lidar sampling for large-area forest characterization: a review. Remote Sens. Environ. **121**(0): 196–209. doi:10.1016/j.rse.2012.02.001.